Proc. Indian Acad. Sci. (Chem. Sci.), Vol. 106, No. 2, April 1994, pp. 303–314.

A "critical" appraisal of electrostatic charge models for molecules

SHRIDHAR R GADRE, SAVITA S PUNDLIK and
INDIRA H SHRIVASTAVA
Department of Chemistry, University of Poona, Pune 411 007, India

Abstract. The conventional electrostatic charge models (PD-AC) are constructed so as to reproduce the molecular electrostatic potential (MESP) on and beyond the van der Waals' (vdW) surface. The MESP distribution has recently [S R Gadre, S A Kulkarni and I H Shrivastava (1992) *J. Chem. Phys.* **96** 5253] been shown to exhibit rich topographical features. With this in view, a detailed topographical comparison of the MESP derived from the charge models, with the respective *ab initio* (MO) ones is taken up for water, hydrogen sulphide, methane and benzene molecules as test cases. It is shown that the point charge models have a fundamental lacuna, viz. they fail to mimic the essential topographical features of MESP. A new model incorporating a small number of floating spherical Gaussians is shown to restore all the critical features of the molecules under study. A comparative study of the standard deviations of MESP derived from charge models on scaled vdW surfaces further reveals that the present model leads to a better representation of *ab initio* MESP.

Keywords. Critical points; topography; electrostatics; charge models.

1. Introduction

Ab initio quantum mechanical methods cannot be readily applied towards a study of interactions between large molecules due to the computational complexities involved. On the other hand, it is known that the electrostatic component of the interaction energies of drugs, biomolecules etc. is a dominant one. With this reasoning, molecular electrostatic potential (MESP) has been utilized to predict sites of electrophilic attack and energy of interaction of polar molecules (Ferenczy *et al* 1990) and in general for a study of non-covalent associations (Naray–Szabo 1993). However, the calculation of *ab initio* MESP is often prohibitive due to the large molecular size or the large number of points over which MESP is to be calculated. A quick and fairly accurate estimation of these electrostatic potentials and interactions is offered in terms of atomic charges (Tomasi *et al* 1991). A wide variety of methods have been designed for obtaining these atomic charges: the well-known popular population analyses by Mulliken (1955) and Löwdin (1950) being the pioneering ones. Other methods of developing net atomic charges include integration of electron density between bond critical boundaries (Bader *et al* 1971), analysis of experimental electron densities (Coppens *et al* 1979) and infrared spectral intensities (Gussoni 1984). The charges derived from Mulliken population analysis are known to be rather unsatisfactory since they fail, in general, to reproduce the electrostatic potential and its derivatives (Williams and Yan 1988). Yet another approach that has been recently developed and which is gaining popularity is the derivation of atomic charges by a least squares fit of the calculated MESP to the quantum mechanically computed MESP (see, for

example, Woods *et al* 1990). These potential-derived atomic charges (PD-AC) which are tailor-made for electrostatic interaction studies, are being widely used since the pioneering work of Momany (1978). The basic idea here is to choose the charges such that they reproduce the quantum mechanical MESP on the van der Waals' (vdW) surface as accurately as possible. A large number of variants (Cox and Williams 1981; Singh and Kollman 1984; Chirlian and Francl 1987; see Reynolds *et al* 1992 for a novel derivation of conformation dependent atomic charges) of the PD-AC-type procedures are now available: the variations essentially being in the choice of points, enforcement of additional constraints, use of different fitting procedures etc. Apart from atom-centred charges, it has been found convenient (see, e.g., Kubodera *et al* 1987) to employ additional point charges at the lone-pair as well as other suitable sites. Such PD-AC's have been incorporated in molecular modelling software packages and generally lead to fairly good predictions of interactions of large molecules.

2. Drawbacks of potential-derived atomic charges

The PD-AC's, as seen in the preceding section, while being able to reproduce the *ab initio* MESP on the vdW surface, have some inherent drawbacks associated with them. For instance, it has been found (Roterman *et al* 1989; Sokalski *et al* 1992) that various popular molecular modelling programs yielded different structures upon optimization of the same protein. The major source of such discrepancies has been traced back to the use of different charge models. Another drawback of these net atomic charges is that they do not always reflect the symmetry of the molecule. Furthermore, the atom-centred point charge models have been observed to be unsatisfactory for some specific cases, particularly for molecules involving lone-pairs (Chipot *et al* 1992).

The PD-atomic charges are obtained by fitting the *ab initio* MESP on or beyond the vdW surface, so that the best fit corresponds to the lowest value of RMSD (root mean square deviation). On the contrary, recent studies (Gadre and Pathak 1990; Gadre and Shrivastava 1991; Gadre *et al* 1992) reveal that the MESP exhibits rich topographical features typically around and beyond the vdW surface. Hence, it was felt that it was worthwhile to undertake a study of the topographical characteristics of the quantum mechanical *vis-a-vis* PD-AC-based MESP. We examine here the water, hydrogen sulphide, methane and benzene molecules and their respective electrostatic charge models as test cases.

3. Charge models for water and hydrogen sulphide

The atom centred models have been found to be unreliable for molecules having important quadrupole moments, such as H_2O and H_2S (Chipot *et al* 1992). Though an inclusion of a charge off the atom has improved the fit for H_2O, in the case of H_2S, the description of charge distribution in terms of monopoles results in large errors in the fitting procedure (Chipot *et al* 1992). Hence, we have chosen these molecules as our first test cases. For both the molecules, the experimental geometry

(Jorgensen 1979 for H_2O and Pietro *et al* 1982 for H_2S) was considered and a 6-31G^{**} basis set taken from a package TURBOMOLE, developed by Ahlrichs and coworkers (Ahlrichs *et al* 1989) employed for the corresponding *ab initio* calculations. The molecular wave functions for these two molecules as well as for the subsequent two test cases are generated employing the *ab initio* package INDMOL (Shirsat *et al* 1993) The critical points (Gadre *et al* 1992b) are isolated and characterized with the help of an efficient parallel program on a 64-node PARAM computer (Shirsat *et al* 1992). The critical points (CP) of a three-dimensional scalar field V are defined as those points where $\partial V/\partial x_i$ $(i = 1, 2, 3)$ are all zero. The non-degenerate CP are those for which none of the eigenvalues of the Hessian $\partial^2 V/\partial x_i \partial x_j$ evaluated at the CP is zero. Such critical points are characterized as (3, + 3) minima, (3, − 1) and (3, + 1) saddles and (3, − 3) maxima.

Recently, a suggestion has been made to devise charge models dictated by MESP-topography (Gadre and Shrivastava 1993). In these models, positive point charges are placed at the nuclear sites supplemented by an appropriate number of spherical Gaussians. The spherical Gaussians are employed to represent the electronic distribution, which is lacking in the PD-AC's. The number of these Gaussians is guided by the number and location of (3, + 3) minima. The parameters are chosen in such a way that *all* the *ab initio* MESP critical points are indeed engendered by the charge model. Further, all the negative MESP-valued CP are fitted quantitatively as closely as possible, to their MO counterparts. A more detailed description of the methodology of deriving these charge models is given in a previous paper (Gadre and Shrivastava 1993). For both H_2O and H_2S, $V(\mathbf{r})$, $\nabla V(\mathbf{r})$ and $\nabla^2 V(\mathbf{r})$ at the negative MESP-valued CPs, are fitted. There are two (3, + 3) CP corresponding to "lone-pairs" with a (3, + 1) saddle point connecting them. Hence, only one (3, + 3) (the other one being symmetry-related) and (3, + 1) CP is fitted in order to develop the charge models.

For the H_2O molecule, a single Gaussian is found sufficient to represent the continuous electronic distribution, centred along the C_2 axis. The exponent of the Gaussian, its centre and the value of the point charges are 'floated' as parameters in the fitting procedure, in order to obtain the best fit. The parameters obtained for the optimal fit are listed in table 1. For the H_2S molecule, a single Gaussian is found inadequate for obtaining two minima (since they are very wide apart) necessitating the use of two Gaussians. This is in conformity with the difficulties associated with a point charge model of this molecule (Chipot *et al* 1992). Here also, the variables are: the Gaussian exponent, centre and the value of the point charges (cf. table 1).

From the result table, it may be seen that the reproducibility of MESP by the charge model developed here is remarkable in terms of the function value, location and the Hessian at the critical points. The positive valued (3, − 1) bond CP (Gadre and Shrivastava 1993) is also reproduced quite close to the *ab initio* one, though the function value is not as comparable. This can be attributed to the low magnitude of the atomic charges employed. On the other hand, *the point charge models must necessarily lack finite valued maxima and minima in V.* This is due to the fact that for point charge models, $\nabla^2 V(r) \equiv 0$ at all the non-nuclear sites: the maxima and minima, on the other hand, demand that $\nabla^2 V$ be strictly negative and positive respectively.

$$\mathrm{RMSD} = \left\{ \sum_{i=1}^{N} (V_i^{\mathrm{mo}} - V_i^{\mathrm{model}})^2 / N \right\}^{1/2}$$

Table 1. MESP topography of *ab initio*[+] (MO) and the present charge model (CM) and the charge model parameters of H_2O and H_2S (values are in a.u.)

Model parameters[a]	Critical point[b]	Location (x, y, z)	$V(\mathbf{r})$	$\nabla^2 V(\mathbf{r})$
H_2O				
	(3, +3) (2)	MO −1·374, −1·779, 0·0	−0·099	0·218
		CM −1·560, −1·618, 0·0	−0·098	0·220
$Ng = 1$	(3, +1) (1)	MO 0·0, −2·286, 0·0	−0·097	0·186
$q_0 = 3·636$		CM 0·0, −2·278, 0·0	−0·097	0·190
$q_h = 0·616$	(3, −1) (2) O–H	MO 0·0, 0·714, 0·913	1·144	5·373
$g_c = 0, 0, 0$		CM 0·0, 0·719, 0·929	0·982	2·316
$g_{exp} = 0·285$; $g_q = -4·868$				
H_2S				
	(3, +3) (2)	MO −3·154, −1·119, 0·0	−0·044	0·080
$N_g = 2$		CM −3·158, −1·119, 0·0	−0·044	0·081
$q_s = 2·981$	(3, +1) (1)	MO 0·0, −3·962, 0·0	−0·0183	0·014
		CM 0·0, −3·931, 0·0	−0·0169	0·009
$q_h = 0·062$	(3, −1) (2)	MO 0·0, 1·197, 1·231	0·811	2·830
	S–H	CM 0·0, 1·463, 1·488	0·334	0·228
$g_c = \pm 0·796, -0·119, 0·0$				
$g_{exp} = 0·159$; $g_q = -1·553$				

[+] The geometry for H_2O was from Jorgensen (1979) and for H_2S from Pietro *et al* (1982). The O and S are at the origin for both H_2O and H_2S. The co-ordinates of H are 0·0, 1·1072, ±1·4304 (H_2O), and 0·0, 1·1752, ±1·8182 (H_2S) respectively.

[a] $Ng \Rightarrow$ number of gaussians; $q \Rightarrow$ charge on nuclei; $g_c \Rightarrow$ Gaussian centre $g_{exp} \Rightarrow$ Gaussian exponent; $g_q \Rightarrow$ charge on Gaussian.

[b] The integers in parentheses denote the type and number of that type of critical point respectively.

[V_i^{mo} and V_i^{model} are the MESP values at the ith point from *ab initio* and the charge model respectively] for the models obtained were calculated on the vdW surfaces. These are compared (cf. table 2) with the RMSD values of the 6–31G** models (PD–AC) proposed by Chirlian and Francl (1987). On comparison it may be observed that the RMSD of the present model is smaller than the PD–AC model on scaled as well as unscaled vdW surfaces. (The vdW radii for H, O and S are 2·27, 2·83 and 3·4 a.u. respectively.) This is despite the fact that the latter model has been derived by fitting MESP on the vdW surface.

In order to vizualize the "goodness" of the MESP on the surface, we have plotted the difference ($V_i^{mo} - V_i^{model}$) on the scaled vdW surfaces. This has been done on a Silicon Graphics workstation, using the graphics vizualization programs developed by Gadre and Taspa (1993). In figure 1, the MESP differences mapped on the scaled vdW surfaces for H_2O molecule is shown. The molecule is viewed along the C_2 axis, from the lone-pair end. Blue colour indicates (numerically) a difference of 10^{-4} to 10^{-3} a.u. and red corresponds to a difference of 10^{-2} to 10^{-1} a.u. It may be seen that the blue region is more extensive in our model (on the RHS of the scale) than in the PD–AC (CF) model for H_2O. This trend is observed on the vdW surface (first pair)

Table 2. Root mean square deviation (RMSD)[a] of MESP on the van der Waals' (vdW) surface and scaled vdW surfaces of the present charge model (CM) and PD–AC (CF)[b] model for H_2O and H_2S.

	H_2O		H_2S	
Scale factor	No. of points	RMS deviation $\times 10^3$	No. of points	RMS deviation $\times 10^3$
1·0	3100	CM 9·18	3476	CM 12·7
		CF 10·6		CF 26·4
1·2	3024	CM 4·73	3308	CM 7·08
		CF 5·91		CF 14·0
1·4	3020	CM 2·80	3208	CM 4·48
		CF 3·95		CF 8·84
1·6	3100	CM 1·88	3132	CM 3·10
		CF 2·87		CF 6·10
1·8	3180	CM 1·38	3088	CM 2·23
		CF 2·13		CF 4·45
2·0	3256	CM 1·09	2952	CM 1·67
		CF 1·61		CF 3·38

[a] See § 3 for definition and details.
[b] The potential-derived charge model reported by Chirlian and Francl (1987).

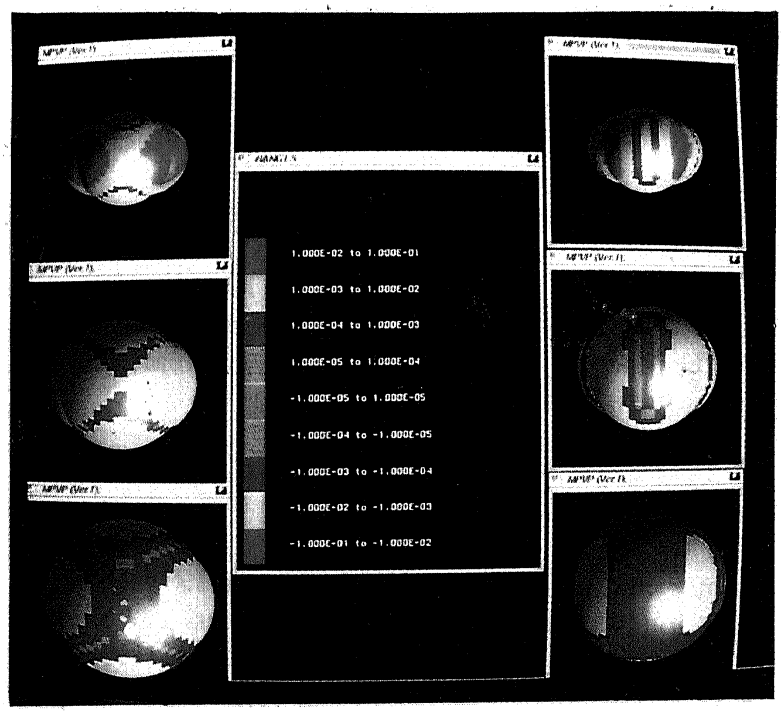

Figure 1. Difference plot of $V(\mathbf{r})$ ($V^{mo} - V^{model}$) on van der Waals' surface, with scale factors 1·0, 1·4 and 2·0 for H_2O. The plots on the left hand side are for the CF model, and those on the right are for the present (CM) model. The plot is viewed along the C_2 axis, from the lone-pair end. (All values in a.u.) The colour assignments are red $\pm 10^{-1}$ to $\pm 10^{-2}$, yellow $\pm 10^{-2}$ to $\pm 10^{-3}$, blue $\pm 10^{-3}$ to $\pm 10^{-4}$, green $\pm 10^{-4}$ to $\pm 10^{-5}$, and pink -10^{-5} to 10^{-5}

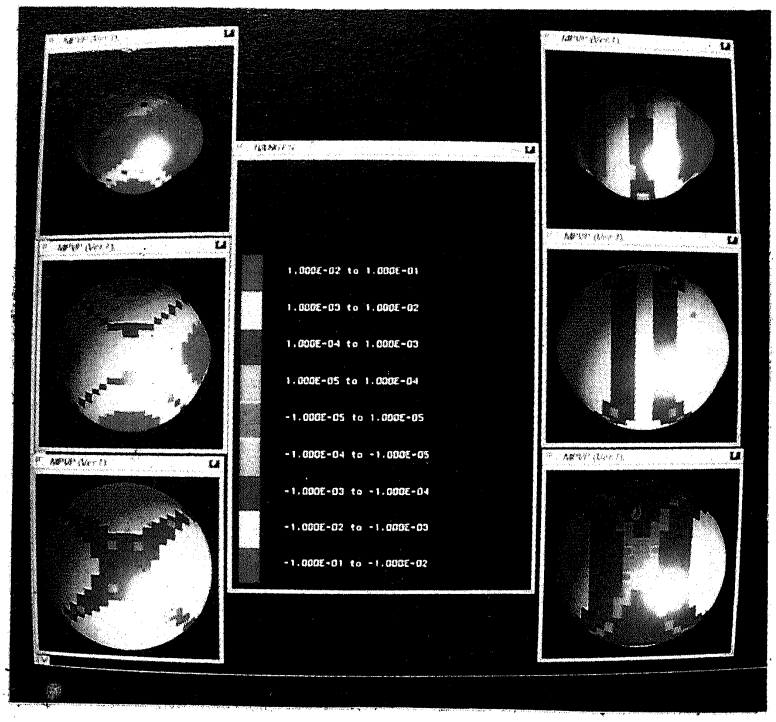

Figure 2. Difference plot of $V(\mathbf{r})$ ($V^{\text{mo}} - V^{\text{model}}$) on van der Waals' surface, with scale factors 1·0, 1·4 and 2·0 for H_2S. The plots on the left hand side are for the CF model, and those on the right are for the present (CM) model. The plot is viewed along the C_2 axis, from the lone-pair end. (All values in a.u.) The colour assignments are red $\pm 10^{-1}$ to $\pm 10^{-2}$, yellow $\pm 10^{-2}$ to $\pm 10^{-3}$, blue $\pm 10^{-3}$ to $\pm 10^{-4}$, green $\pm 10^{-4}$ to $\pm 10^{-5}$, and pink -10^{-5} to 10^{-5}

as well as on its scaled versions (cf. table 2). For H_2S (figure 2), our model shows an even better fit in the lone-pair region, as compared to the corresponding CF model. Also, the fit is seen to improve in our model (on the RHS of the scale), as the scale factor (second (1.4) and third (2.0) pair) is increased (cf. table 2). Thus it may be seen, that the MESP in the lone-pair region is particularly well represented by our model in both the cases considered here.

4. Charge models for methane and benzene

For the methane molecule, an SCF calculation using a TZ2P (Ahlrichs *et al* 1989) basis has been carried out by using the experimental (Synder and Basch 1972) geometry and employing the parallel package INDMOL (Shirsat *et al* 1993). For benzene, the geometry reported in a previous study (Gadre *et al* 1992b) has been employed with a TZP (Ahlrichs *et al* 1989) basis set. For these two molecules, the same procedure as discussed above has been used. viz. the negative valued CP's are fitted. Due to the inherent symmetry of CH_4 and C_6H_6, a fitting of only one and two negative MESP valued CP's respectively suffices. For C_6H_6, 12 Gaussians are required (6 above the ring plane and 6 below), whereas for CH_4 only a single Gaussian at the carbon nucleus is found to be adequate. Further, all the nuclei carry positive charges

and yield a (3, − 1) in between the bonded ones. Figure 3a displays the *ab initio* (MO) MESP of the methane molecule in a plane containing the S_4 axis and bisecting the H–H lines perpendicularly. In the contour maps presented here, the solid and dashed lines represent the positive and negative MESP values respectively. A CP is indicated either by an asterisk or a cross, as the case may be. The most prominent feature for methane is the existence of the negative valued (3, + 1) type saddles (Gadre *et al* 1992b) along the C_2 axes (6 of them, out of which 4 are noticeable in figure 3a). The MESP inside a cube of side (≈) 2·6 Å centred on the carbon atom, is strictly positive. Now compare and contrast the critical features of MESP derived from the point charge model (PD–AC) for methane molecule (cf. figure 3b) employing the 6–13 G** charges due to Chirlian and Francl (1987). This PD–AC model fails to reproduce *any finite-valued CP whatsoever*, evidently, due to *complete lack* of representation of the continuous distribution. In fact, the detailed features of PD–AC MESP are grossly different from its MO counterpart (cf. figures 3a and b). The MESP in the region close to the carbon atom is negative in the PD–AC model (figure 3b) which is in direct contrast to the corresponding MO one. Moreover, a detailed study of the topography of MESP of the PD–AC model, reveals no trace of a positive MESP valued (3, − 1) bond CP between C and H atoms which is an essential feature of a bond (Gadre *et al* 1992b). Note, however, that the two figures show a good match *on the vdW surface*: the negative values along the axes as well as the positive values along the diagonals. This example clearly brings out how similar two scalar fields may appear when viewed only on a surface and yet be so different in three dimensional space! In contrast, the topographical features of MESP are very well-reproduced by

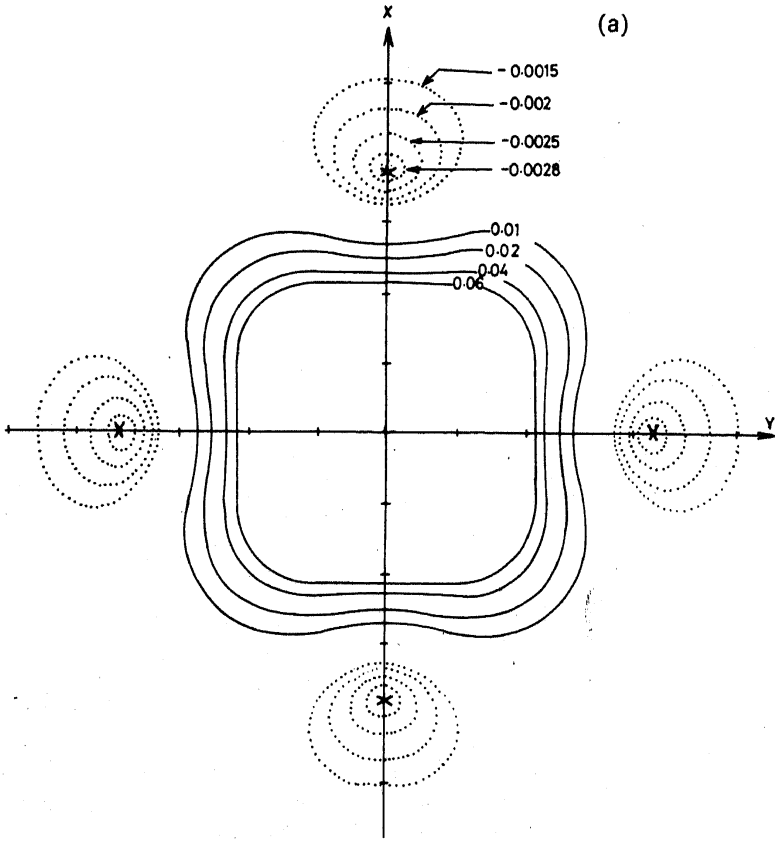

Figure 3. (a) (Caption on next page.)

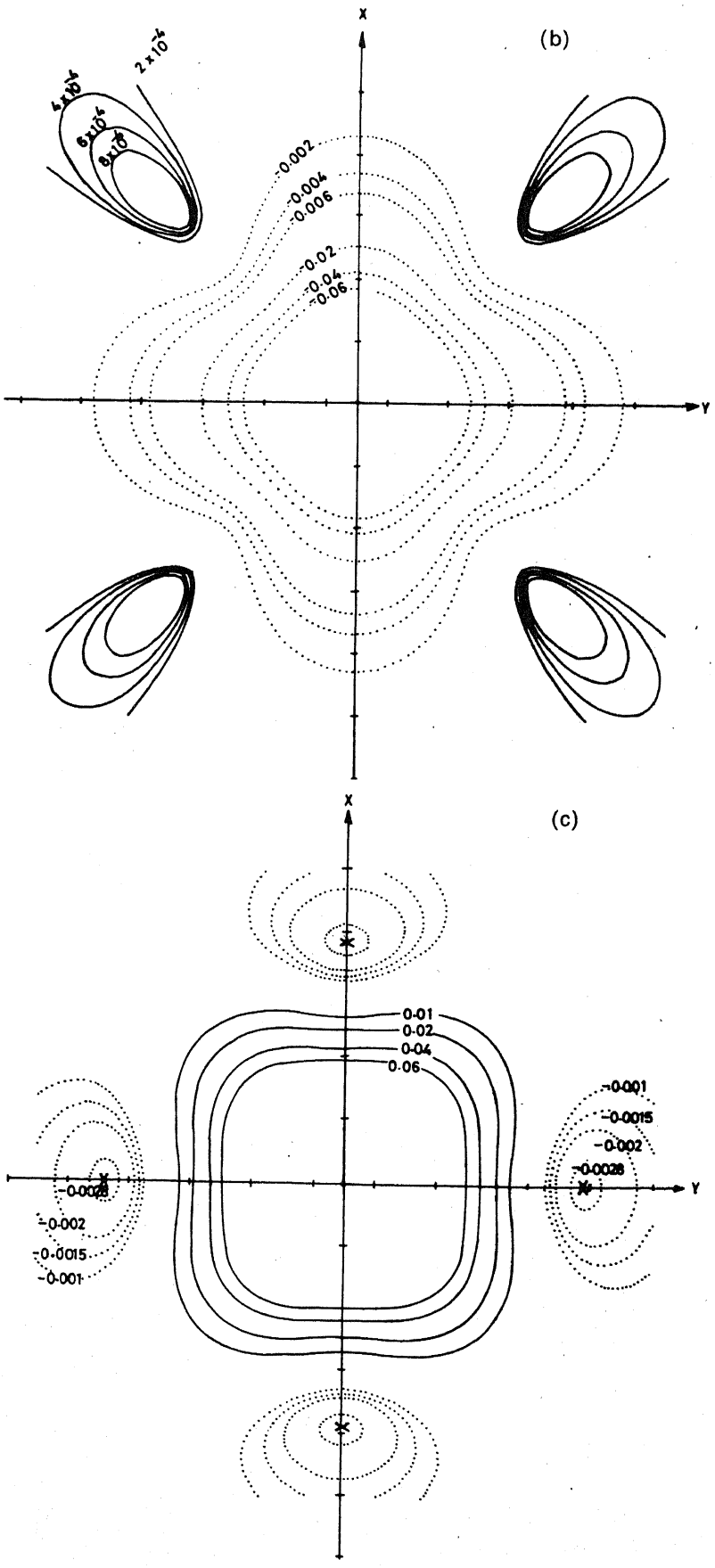

Figure 3. MESP contour map of CH_4 in a plane containing the C nucleus and bisecting the H–H lines. X's indicate (3, +1) saddle points. (All values in a.u.). (**a**) *Ab initio* MESP. (**b**) PD–AC MESP. (**c**) Charge model MESP.

our model (figure 3c). Both the positive as well as the negative regions of the *ab initio* MESP are mimicked extremely well by the model developed in the present work by fitting *only some CP's* in the MESP topography. A remarkable feature of this model is that it has been obtained by fitting only one negative MESP valued (3, + 1) CP for CH_4.

The situation is quite similar for the benzene molecule, the computational details of which are similar to those for methane. The MO MESP depicted in figure 4a exhibits a rich topography on a plane perpendicular to the plane of the ring and bisecting two opposite C=C bonds. The (3, + 3) minima indicated by asterisks, represent the π bond-pair and the saddles indicated by crosses, represent (3, − 1) CP's. The STO–3G PD–AC (Kubodera *et al* 1987) on the other hand (cf. figure 4b), completely fail to exhibit even the overall qualitative features. The MO MESP is *exclusively positive* in the ring whereas the PD–AC–MESP is *negative* in the ring plane excluding a small positive-valued island at the centre. Though there is a (3, − 1) CP on the C_6 axis around 1·46 Å from the centre (figure 4b), the negative-valued minima are conspicuous by their absence. Nonetheless, the match of the MESP on the vdW surface is indeed very good here as well. The chief reason for the gross mismatch of topographical features of PD–AC MESP's with their MO counterparts is that *in the former the continuous component* (Hall 1986) *viz. the electron density is not represented at all.* From the MESP contour map of our benzene charge model (figure 4c), as well as the results discussed in table 3, it can be seen that the qualitative features are quite well-reproduced in the negative MESP region for both the test cases. The positive MESP region, due to the low magnitude of the point charges,

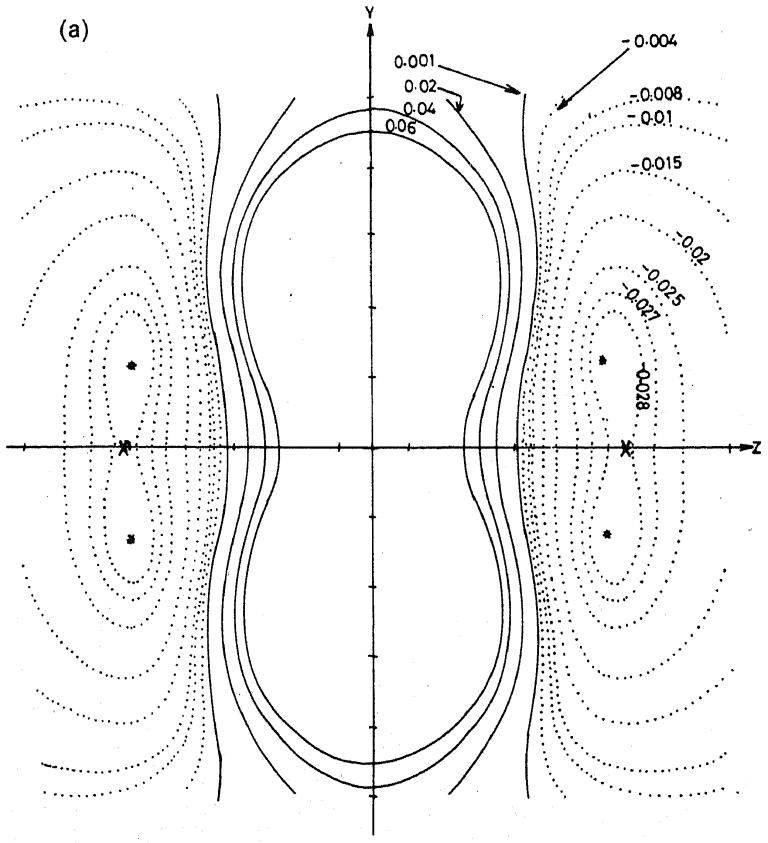

Figure 4. (a) (Caption on next page.)

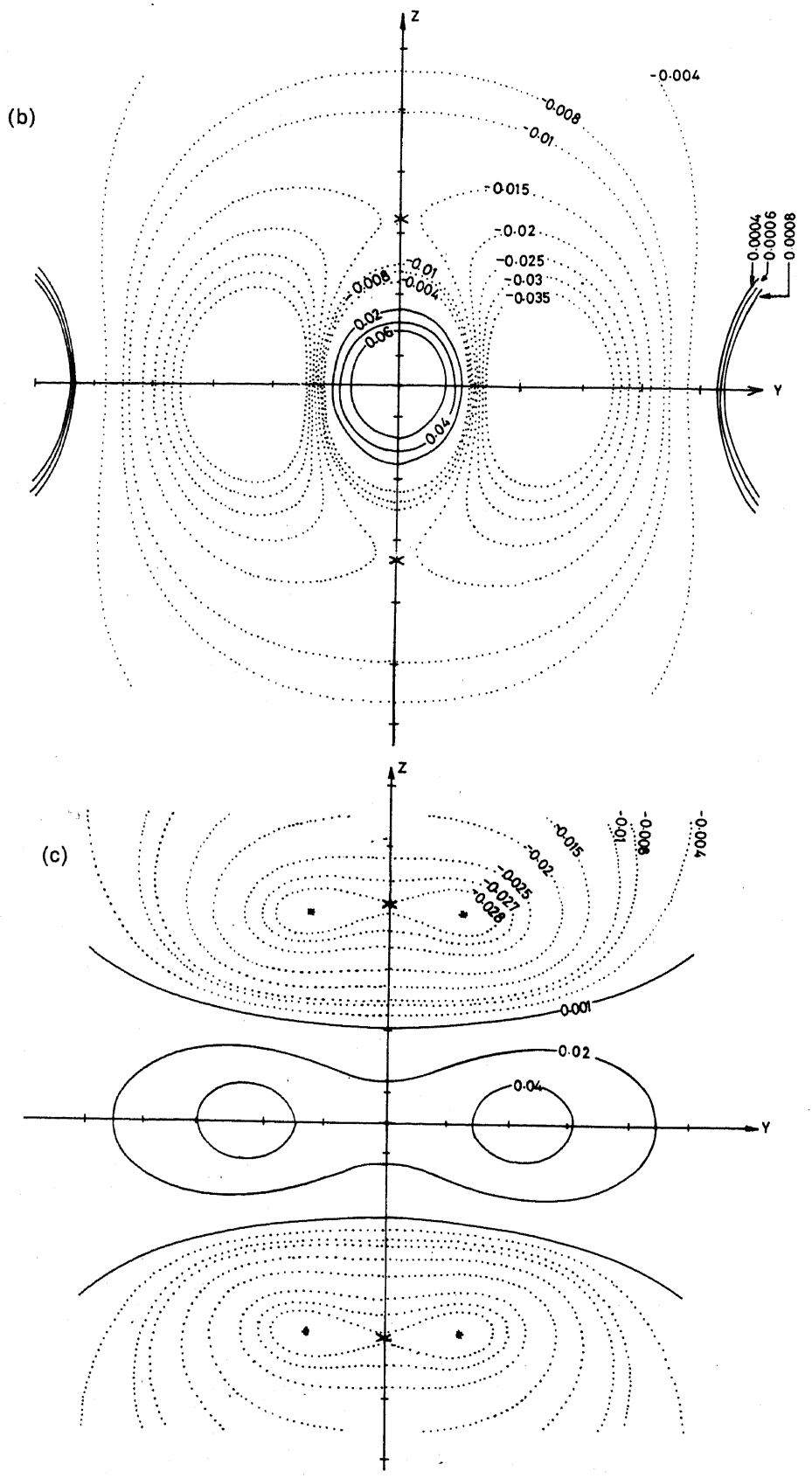

Figure 4. MESP contour map of C_6H_6 in a plane perpendicular to the plane containing the ring and bisecting two opposite C=C bonds. The *'s indicate the (3, + 3) minima and X's indicate the (3, + 1) saddle points. All values in (a.u.) (**a**) *Ab initio* MESP (**b**) PD–AC MESP (**c**) Charge model MESP.

Table 3. MESP topography of *ab initio*[+](MO) and the present charge model (CM) and the charge model parameters of CH_4 and C_6H_6 (values are in a.u.)

Model parameters[a]	Critical point[b]	Location (x, y, z)		$V(\mathbf{r})$	$\nabla^2 V(\mathbf{r})$
CH_4					
$Ng = 1$	(3, +1) (6)	MO	3·794, 0, 0	−0·00292	0·014
$q_c = 0{\cdot}891$		CM	3·794, 0, 0	−0·00294	0·014
$q_h = 0{\cdot}227$	(3, −1) (4)	MO	0·754, 0·754, 0·754	0·833	3·615
$g_c = 0, 0, 0$		CM	0·754, 0·754, 0·754	0·348	0·330
$g_{exp} = 0{\cdot}124$, $g_q = -1{\cdot}802$					
C_6H_6					
$Ng = 12$	(3, +3) (12)	MO	1·089, 0·629, 3·408	−0·02899	0·0207
$q_c = 0{\cdot}0526$		CM	1·089, 0·629, 3·408	−0·02899	0·0208
$q_h = 0{\cdot}0166$	(3, +1) (12)	MO	1·187, 0, 3·421	−0·02893	0·0194
		CM	1·187, 0, 3·421	−0·02893	0·0192
	(3, +1) (1)	MO	0, 0, 0	0·161	0·288
		CM	0, 0, 0	0·0256	0·0003
$g_c = 0, 2{\cdot}257,$	(3, −1) (2)	MO	0, 0, 3·510	−0·0282	0·0089
2·742		CM	0, 0, 3·504	−0·0281	0·0089
		PDAC[c]	0, 0, 2·766	−0·0156	0·0
	(3, −1) (6)	MO	0, 2·252, 0	0·905	4·137
$g_{exp} = 0{\cdot}283$	C=C	CM	0, 2·274, 0	0·0502	0·001
$g_q = -0{\cdot}0346$	(3, −1) (6)	MO	3·90, 0, 0	0·877	3·801
	C–H	CM	3·90, 0, 0	0·0484	0·0001

[+] The geometry for CH_4 was from Snyder and Basch (1972). The C is at the origin, and the co-ordinates of H are ±1·818, ±1·818, ±1·818 (signs chosen appropriately). For C_6H_6, the D_{6h} geometry was the TZP (Ahlrichs *et al* 1989) optimized one. The C=C and C–H bond lengths are 2·607 a.u. and 2·023 a.u., respectively, the Z axis being the C_6 axis.

[a,b] The notations are as in table I.

[c] PD–AC ⇒ Point charge model reported by Kubodera *et al* (1987).

does not compare *quantitatively* with the corresponding MO one, though the critical features, viz. the (3, −1) bond CP's are indeed observed in the neighbourhood of the corresponding MO ones (cf. table 3) for the methane as well as benzene molecules. It may be worthwhile employing such a topography-driven model for studying the stacking problem of benzene molecules as recently studied by Hobza *et al* (1993).

5. Conclusions

In summary, the conventional point charge models have a major fundamental lacuna, viz. they fail to mimic the essential topographical features of MESP. Addition of any further point charges (e.g. at the lone-pair sites) does not alleviate this shortcoming. Our new model rectifies this situation by fitting the MESP, field and Hessian exclusively at the negative-valued MESP critical points. This successfully restores all the essential topographical features observed in the corresponding quantum mechanical MESP. Moreover, the charge model developed in the present work also shows a better representation of the MESP on the vdW as well as scaled vdW surfaces, as compared

to their more traditional PD–AC counterparts, in spite of the fact that the latter are developed by fitting the MESP on the vdW surface. Such charge models faithfully representing topography are *expected to yield* better directional characteristics and eventually turn out to be better candidates for studying molecular interactions. Further work in this direction is under way in our laboratory.

Acknowledgements

Thanks are due to Professor Uri Dinur for useful suggestions regarding this work. The financial assistance from the Department of Science and Technology, New Delhi, and the Centre for Development of Advanced Computing (C–DAC), Pune is gratefully acknowledged.

References

Ahlrichs R, Bär M, Häser M and Kölmel C 1989 *Chem. Phys. Lett.* **162** 165
Bader R F W, Beddall P M and Cade P E 1971 *J. Am. Chem. Soc.* **93** 3095
Chipot C, Maigret B, Rivail J-L and Scheraga H A 1992 *J. Phys. Chem.* **96** 10276
Chirlian L E and Francl M M 1987 *J. Comput. Chem.* **8** 894
Coppens P, Guru Row T N, Leung P, Stevens E D, Becker P J and Yang Y W 1979 *Acta Crystallogr.* **A35** 63
Cox S R and Williams D E 1981 *J. Comput. Chem.* **2** 304
Ferenczy G G, Reynolds C A and Richards W G 1990 *J. Comput. Chem.* **11** 159
Gadre S R, Kölmel C and Shrivastava I H 1992a *Inorg. Chem.* **31** 2279
Gadre S R, Kulkarni S A and Shrivastava I H 1992b *J. Chem. Phys.* **96** 5253
Gadre S R and Pathak R K 1990 *Proc. Indian Acad. Sci. (Chem. Sci.)* **102** 189
Gadre S R and Shrivastava I H 1991 *J. Chem. Phys.* **94** 4384
Gadre S R and Shrivastava I H 1993 *Chem. Phys. Lett.* **204** 350
Gadre S R and Taspa A 1993 *J. Mol. Graph.* (in press)
Gussoni M 1984 *J. Mol. Struct.* **115** 307
Hall G G 1986 *Int. J. Quantum Chem.* **5** 115
Hobza P, Selzle H L and Schlag E W 1993 *J. Phys. Chem.* **97** 3937
Jorgensen W L 1979 *J. Am. Chem. Soc.* **101** 2011
Kubodera H, Nagakawa S and Umeyama H 1987 *Chem. Pharm. Bull.* **35** 1673
Löwdin P-O 1950 *J. Chem. Phys.* **18** 365
Momany F A 1978 *J. Phys. Chem.* **82** 592
Mulliken R S 1955 *J. Chem. Phys.* **23** 1833
Naray-Szabo G 1993 *Chem. Design Autom. News* **8** (May) 1
Pietro W J, Francl M M, Hehre W J, Defrees D J, Pople J A and Binkley J S 1982 *J. Am. Chem. Soc.* **104** 5048
Reynolds C A, Essex J W and Richards W G 1992 *J. Am. Chem. Soc.* **114** 9075
Roterman I K, Gibson K D and Scheraga H A 1989 *J. Biomol. Struct. Dyn.* **7** 391
Shirsat R N, Bapat S V and Gadre S R 1992 *Chem. Phys. Lett.* **2** 373
Shirsat R N, Limaye A C and Gadre S R 1993 *J. Comput. Chem.* **14** 445 (the parallel SCF package INDMOL, developed by S R Gadre and co-workers)
Singh U C and Kollman P A 1984 *J. Comp. Chem.* **5** 129
Sokalski W A, Shibata M, Ornstein R L and Rein R 1992 *J. Comput. Chem.* **13** 883
Synder L C and Basch H 1972 *Molecular wave functions and properties* (New York: Wiley)
Tomasi J, Bonaccorsi R and Cammi R 1991 *Theoretical models of chemical bonding* Z B Maksic (Berlin, Heidelberg: Springer) Part 4
Woods R J, Khalil M, Pell W, Moffat S H and Smith V H Jr 1990 *J. Comput. Chem.* **11** 297
Williams D E and Yan J M 1988 *Adv. At. Mol. Phys.* **23** 87